Extensive Air Showers (HE-4)

R.W. Clay
Physics Department
University of Adelaide
North Terrace
ADELAIDE South Australia 5001

1. Introduction

At the conference I felt that air shower work had made genuine progress particularly due to the professionalism of work at the large arrays. More than ever, those using medium sized arrays have to be selective in their work and careful in their analysis when shower information is incomplete. Ultra high energy gamma-ray astronomy is an exciting new area for us and has added a new sense of purpose to ground based array work. There is much to be done before we properly understand U.H.E. gamma ray showers and it is important that we remain conservative with our claims whilst the properties of such showers are still not clear. Their muon content is only one of the properties to be clarified by the next conference.

There seems to have been genuine progress on primary composition. When allowance is made for detection effects there is impressive agreement on mean depths of maximum at fixed energy. It remains to be seen how well we can now progress to the second order problem of detailed interaction parameters once the gross features of our beam are clarified (see eg. Wrotniak and Yodh HE 4.1-2).

The shower disk thickness has become an area of intense study with interest in Linsley's technique for measurements of giant showers (which should have its uses but is not a complete self-contained solution to spectra and anisotropies at 10^{20} eV) and in the study of structure near the core for improving fast timing and studying delayed sub-showers.

Perhaps the most significant area of promise for the future is the study of individual shower developments with Cerenkov and, particularly, air fluorescence techniques. The importance and potential of having relatively complete information on a complete set of individual showers can hardly be overestimated. However, we must also have a complete understanding of the observation process; why we observe the showers we do and whether or not the recorded data set is complete at a given energy, apparent core distance, and zenith angle.

2. Shower Observations

Extensive air showers are usually studied with ground based detectors in arrays which first detect the presence of a shower and are then used to study a set of shower parameters. The showers are classified and ordered to give information about some parameter or about how that parameter depends on another shower property, perhaps shower size or primary energy. Unfortunately, air showers are complex and, as a general rule, the set of showers which is observed is less complete than we would like. Thus, data sets invariably contain bias in their selection and great care must be exercised when interpreting the data, particularly when mean values of parameters are derived. In some cases, intuition and experience are barely sufficient to picture the unbiased original data set

from the data which are presented and the results may then only properly be understood when compared to simulations of the whole air shower/array detection procedure.

These problems were an underlying theme in a number of areas addressed at the conference. In particular, the difficulty of comparing data obtained in terms of a shower size with data presented in terms of a primary energy was particularly apparent. The problem is usually not so much in measuring the parameters of interest but in understanding how the detection system sampled the incoming set of air showers and how the final data set was selected.

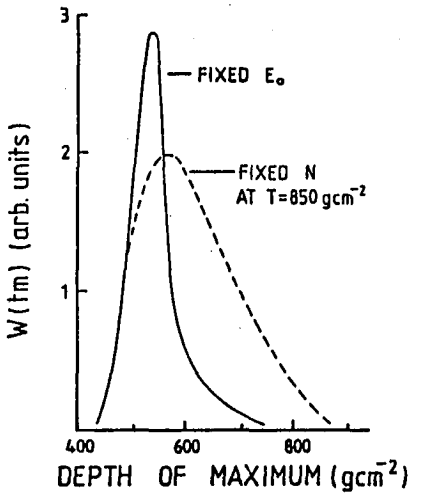

Fig 1. The difference in distributions of observed depths of maximum when shower selection is by fixed primary energy and fixed shower size. (HE 4.1-20)

Shower Size and Primary Energy

Shower size has serious limitations for use as a parameter for ordering showers in energy due to the combination of shower fluctuations and a steeply falling primary energy spectrum. Air shower arrays often trigger on particles which reach the detection level and the resulting observed distribution of showers can then be close to complete in Ne but not in primary energy. One usually wants data measured at fixed primary energy and, without further development information, the interpretation of observations can be seriously in error.

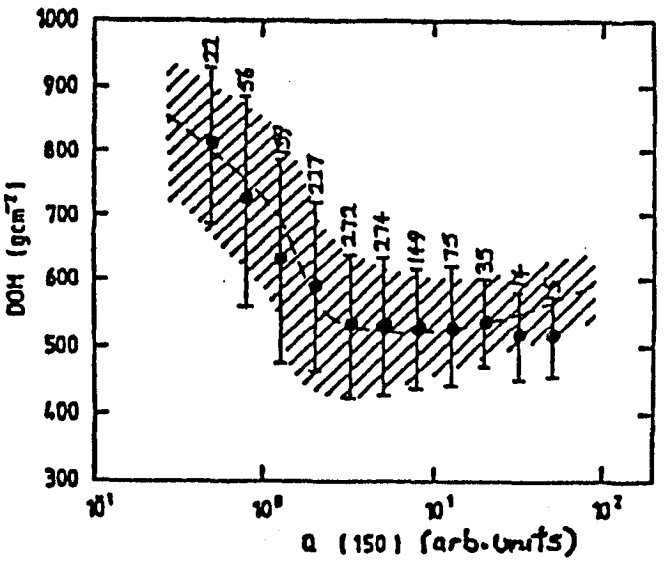

Fig 2. Experimental distribution of depth of maximum vs primary energy estimator Q(150). The hatched region is for simulated data. (OG 5.2-11)

An example of the difference between measurements in terms of primary energy and shower size is shown in figure 1 (from HE 4.1-20) where it is clear that a mean depth of shower maximum in terms of fixed primary energy

will be quite different to a mean derived for a fixed shower size; differences of up to 200 g cm^{-2} are possible. Calculations in OG 5.2-11 show other aspects of the selection of showers by real particle arrays. In terms of fixed primary energy, figure 2 shows a clear tendency to select only downward fluctuating (late developing) showers close to the array size threshold (which can be set not only by the hardware triggering but also by a software trigger if this is based on a size parameter). Also, since the energy spectrum is steep, any data set will consist preferentially of downward fluctuating low energy showers so that the system will emphasise any shower effects associated with downward fluctuations. This applies particularly if the composition of the primary beam at constant energy contains a mixture of nuclei.

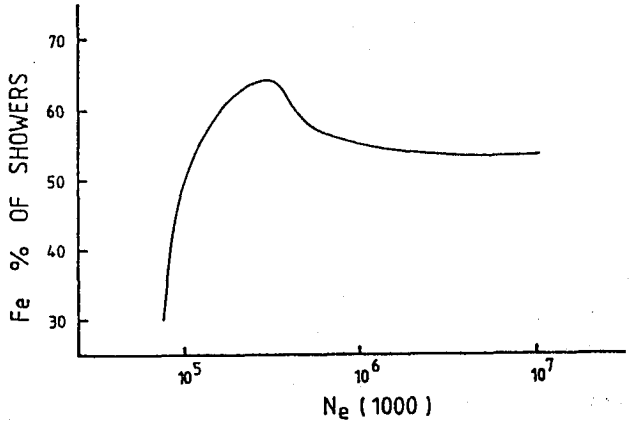

Fig 3. The fraction of all analysable sea level showers produced by iron primaries, as a function of $N_e(1000)$, for a composition of 90% Fe and 10% p. (B.R. Dawson, private communication)

In this case, proton initiated showers with their long interaction mean free path and large fluctuations will be preferentially selected. This effect is shown in figure 3 where the apparent fraction of protons in the beam is seen to be considerably enhanced when recorded by a typical array.

3. Depth of Shower Maximum

The depth of shower maximum and its fluctuations are important parameters in the studies of primary particle composition and the early shower interaction processes. Early cascade maxima are associated with short primary particle mean free paths and high secondary particle multiplicities. Similarly, small fluctuations in the depth of maximum are also associated with short mean free paths since these fluctuations largely mirror fluctuations in the depth of the first interaction. Convention has it that proton primaries are associated with long mean free paths ($\gtrsim$ 80g cm^{-2}) and large fluctuations and "iron" primaries have short mean free paths ($\lesssim$ 20g cm^{-2}) and small fluctuations. The real primary beam will probably be a mixture of species and one would wish to at least determine whether the beam is "iron dominated" or "proton dominated" at a given energy.

A substantial amount of new information on depths of maximum became available at the conference, both theoretical and experimental. These data are summarised in figures 4 and 5. The theoretical work (fig. 5) clearly confirms that the composition of the initiating particle is the major factor affecting the depth of maximum and it should be possible to interpret the experimental data in terms of composition with some confidence since the separation of the composition lines is large compared to the expected experimental errors for individual events

($\lesssim 30 g cm^{-2}$, HE 4.4-16) .

Figure 4 summarises the position on shower depths of maximum with particular reference to recent results. The data from ~ 10^{15}eV to 10^{19}eV appear to follow a consistent relationship and general agreement is remarkably good considering the variety of techniques used to obtain these data. Some comments on the experiments are necessary since some of the spread in the data is due to instrumental and technique effects.

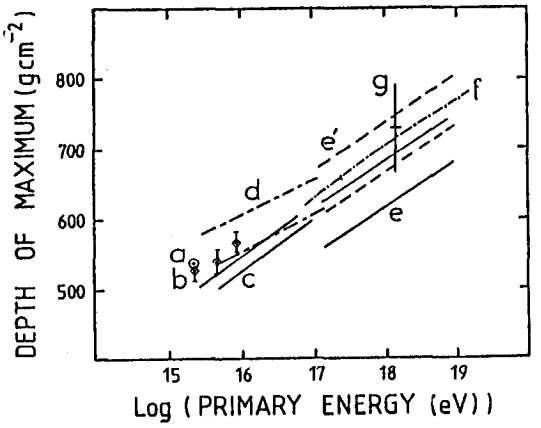

Fig 4. Measured depths of shower maximum.

(a) HE 4.4-13 (b) HE 4.4-15.
(c) OG 5.2-11 (d) Inoue et al. (1985)
(e) HE 4.1-19 (e') Before sub of 50g cm^{-2}
(f) OG 5.1-13 (g) OG 5.1-7

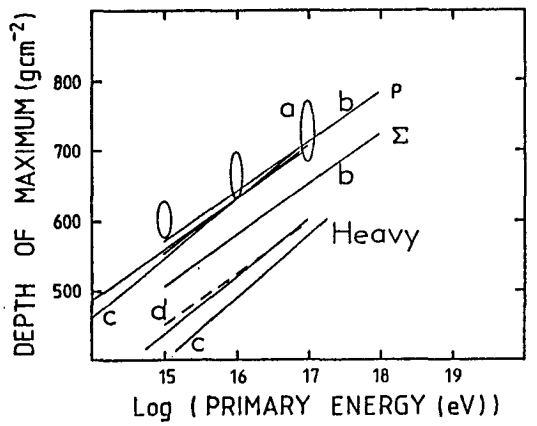

Fig 5. Theoretical Depths of Shower Maximum

(a) HE 4.1-2 (b) HE 4.4-15
(c) HE 4.1-10 (d) OG 5.2-11

The Samarkand array provides us with data at the lowest energies (HE 4.4-13). The array was used to select showers on the basis of their Cerenkov light. This provides a trigger which should approximate directly to a primary energy trigger since we expect the Cerenkov light flux at $\gtrsim$ 100m from the core to be a good primary energy estimator (fig. 6) and these should be typical core distances for the triggering detectors. In constrast, the Cerenkov flux on axis is a good measure of the ground level shower size and so the Cerenkov lateral distribution function clearly reflects shower development. The lateral distribution function can be well approximated by a simple exponential of the form $q(r) \sim \exp(-br/10^4)$ and the parameter b is thus a sensitive measure of shower development (fig. 7).

The Samarkand workers interpreted their data by simulating their experimental data with a particular composition and interaction model and showed that their experimental and simulated data fitted well at 2×10^{15}eV although their

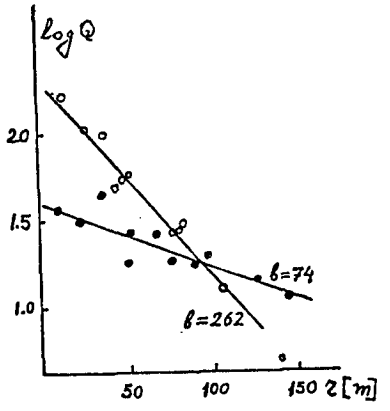

Fig 6. Cerenkov light lateral distributions for $E_0=3x10^{15}$eV but different depths of maximum. (HE 4.4-13)

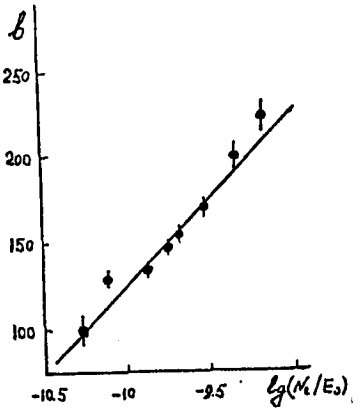

Fig 7. The relationship between the Cerenkov lateral distribution parameter b and a known depth of maximum parameter N_e/E_0. (HE 4.4-13)

observed fluctuations in depth of maximum were probably not sufficient with this model. It is not easy to judge the sensitivity of the fit between experiment and simulation to variations in the model. It is thus important that when experiments are compared to models, some measure of model sensitivity is explicitly stated. If the calculations of Patterson and Hillas (1983) are applicable at the Samarkand altitude, it is likely that the use of the Cerenkov flux at 100m from the core will cause a slight overestimate ($\sim 10 g cm^{-2}$) of the depth of maximum since the flux only becomes a really satisfactory primary energy parameter for r ~ 150m.

A similar comment might also apply to the other Samarkand result (HE 4.4-15) shown in fig. 4 since this uses the same primary energy estimator. In this case, the Cerenkov pulse shape was studied and depths of maximum at fixed primary energy were obtained which were rather higher in the atmosphere than before when a less satisfactory primary energy estimator had been used. Cerenkov pulse shape measurements are potentially very powerful but, since a great deal of information must be extracted from single pulses, they are very susceptible to selection problems and are technically demanding (see eg, Liebing et al 1984, Inoue et al 1985a). In order to be recorded, a pulse must be of a suitable amplitude and, for a given total pulse area (Cerenkov flux), this amplitude depends on shower development. A selection was made of a total of 83 events for analysis out of a recorded data set of 4000 showers. In principle, this technique of a posteriori selection of an unbiased data set is acceptable but one needs to be sure that no physics is being lost in the process. The great potential of the pulse shape technique is in its sensitivity to early shower development unlike lateral distribution experiments which are more sensitive to the cascade development past maximum. However, very good

instrumental dynamic range and wide bandwidths are necessary.

The Adelaide group (OG 5.2-11) also presented Cerenkov lateral distribution results. They interpreted their results with simulations and fitted a mixed composition model over a decade in energy. In this case, both the depth of maximum and its fluctuations seemed to be fitted by the model and the spread of acceptable models was 85-95% iron plus protons. This mixture becomes only ~50% iron in the observed beam at fixed shower size at ground level. The Adelaide data did not give such a good fit to the Samarkand composition of 40% protons plus 15% each of A = 4, 15, 31, and 56 (B.R. Dawson, Private communication) but, at this stage of sophistication, particular interaction models and detailed theory relating the lateral distribution function to development must also become important.

Inoue et al (1985a,b) have recently presented Cerenkov results from the Akeno and Chacaltaya arrays. These data are included in the figure after a conversion from their Ne to primary energy using Akeno size and energy spectrum results. Such a procedure is dangerous and has been used only since the results then represent upper limits as indicated in the original paper. Based on experience, one might expect depths of maximum to be overestimated by $\lesssim$ 50g cm^{-2} through the use of a shower size trigger and later conversion to primary energy.

Above 10^{17} eV, two data sets were presented at the Conference, by Dyakonov et al (OG 5.1-13) and by Glushkov et al (HE 4.1-19). The former data were derived from mean Cerenkov lateral distributions in a number of energy intervals obtained at Yakutsk and the latter were from a new analysis of a broad range of development-dependent parameters (electron lateral distribution function, Cerenkov light to electron ratio, and electron to muon density ratio at 300m from the core) measured at Yakutsk. Some of these parameters allowed a determination of depths of maximum in rather model independent ways (fig 8). The results were obtained in terms of fixed size parameter $\rho_s(300)$ and the authors comment that at fixed E the values of X_{max} would be ~ 50g cm^{-2} less. This correction is included in the diagram. It is not clear whether or not the work of Dyakonov et al should include a similar correction since this depends on the precise way in which shower selection and averaging were carried out.

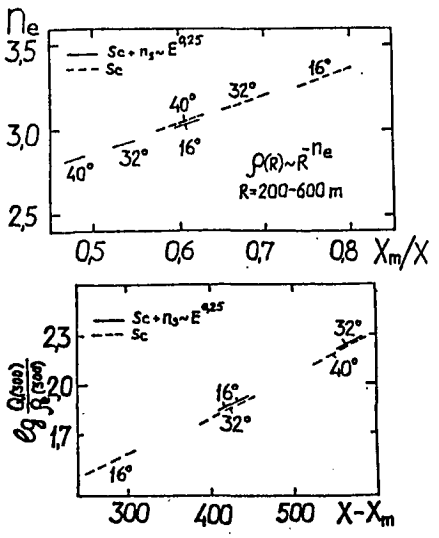

Fig 8. Relating the electron lateral distribution and the ratio of Cerenkov light to electrons (at 300m) to shower development. (HE 4.1-19)

Theory predicts such a large separation of depths of maximum of iron and proton showers that it should be possible to significantly improve our estimates of composition at fixed primary energy by looking at the actual distribution of depths in very limited energy ranges in a way

similar to that used by Nikolsky et al (1981) (see also OG 5.2-5) for fluctuations of Nμ and Ne. The resolution should be quite good with the Cerenkov techniques and sufficient events are probably already available at Samarkand and Adelaide.

Fluctuations in the Depth of Shower Maximum

Fluctuations in the depth of shower maximum should reflect primary composition through the large difference in the interaction mean free path of protons and heavier primaries. Heavy primaries should have much smaller fluctuations in depth of maximum ($\lesssim$ 30g cm^{-2}) than protons ($\sim$ 60g cm^{-2}). It is interesting that $\sigma_{x_{max}}$ can be measured through analyses of variance without a direct measurement of x_{max}. Figure 9 summarises data presented at the conference. The data favour proton like fluctuations. However, similar results would be obtained for a mixed composition, and it is unlikely that this technique is powerful except for eliminating the possibility of a pure iron primary beam (or at least lacking in light nuclei). It is interesting to see that the fluctuations at the highest energies are reduced, as one would expect for cross sections which increase appreciably with energy.

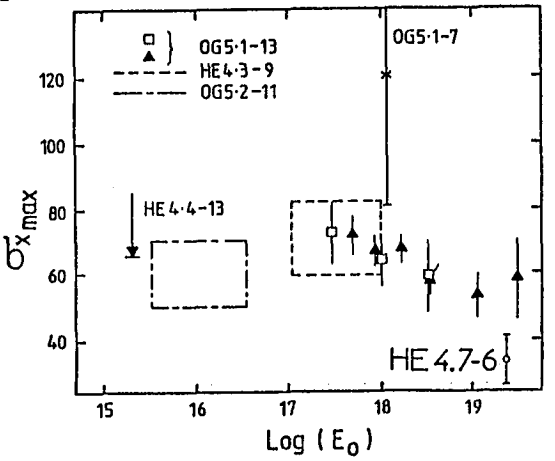

Fig 9. Fluctuations in shower depth of maximum.

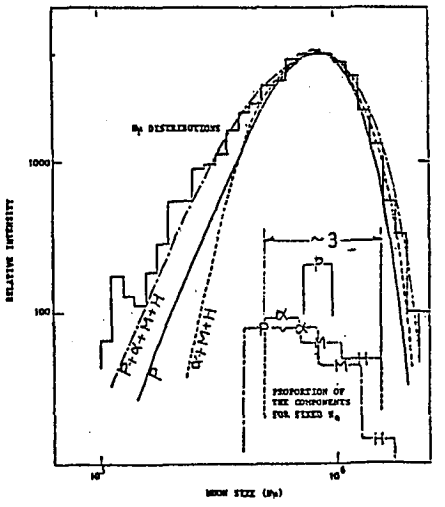

Fig 10. Observed and calculated distribution of muon size for fixed N_e. (HE 4.1-3).

There are some other results which require at least some protons in the primary beam. These are measurements of muon size at fixed Ne from Akeno (HE 4.1-3) analysed by Tanahashi which show a long tail at small Nμ due to the fluctuations of a proton component (fig 10). Also, equi-intensity cuts show a long shower attenuation length which is probably due to the large proton shower fluctuations. As a general comment on cascades discussed at the conference it is noteworthy that the cascade attenuation lengths of $\sim$ 200g cm^{-2} found with equi-intensity cuts should represent conservative upper limits to the single cascade proton development curves. A number of workers have been using much longer attenuation lengths in their models which would seem to be inappropriate.

4. Novel Techniques for the Economical Study of Giant Showers

Arrays which are used to study the very highest energy showers have now accumulated data with ~ 10^3 km^2 yrs collection in both northern and southern hemispheres. There are many questions of composition, interaction properties, anisotropy, and spectra which remain controversial or virtually undiscussed at these energies and a good case can be made for experiments which might expect to increase the data accumulation by a factor of ten in a reasonable time and at a reasonable cost. Modestly priced arrays with collecting areas of ~ 10^3 km^2 at 10^{19} eV are required. Such arrays were described at the conference using air fluorescence techniques, radio techniques, or by measuring the longitudinal thickness of the shower front at large core distances. There is potential in each technique but, though each may find its place in overall systems, none seems to be a single satisfactory answer to the replacement of conventional systems in a new generation of arrays.

The Longitudinal Thickness of the Shower Front

The thickness of the shower disk has been the subject of continuing but not major study for a number of years. It has been relevant to radio studies, fast Cerenkov studies, and particularly the risetime studies of the Haverah Park group. Recently there has been an increase in interest in this area due to a suggestion by Linsley (1983) that this parameter might be a useful direct measure of core distance thus enabling cheap EAS arrays to be built with large collecting areas for the study of giant air showers. It may not then be necessary to enclose the shower collecting area with detectors in order to obtain a useful shower analysis. In terms of shower studies, this section of the conference was unique in the sense that it was completely experimental in its outlook.

Linsley has shown (and extended his discussion here) that the thickness of the shower front can usefully be expressed as a dispersion $\sigma_t = [\int (t-\langle t\rangle)^2\, p(t)\, dr]^{0.5}$ and that as, a function of core distance, this is given by $\sigma_t \simeq \sigma_{to}\ (1+r/r_t)^b$ where σ_{to} = 2.6ns, r_t = 30m and b ~ 1.5 (or for for practical purposes a weak function of zenith angle described at the conference (HE 4.7-14)). Investigations of σ_t were presented and the extent of its usefulness was discussed in comparison with data from conventional array analyses together with specific proposals for "mini-arrays" to detect giant air showers using the "Linsley" method.

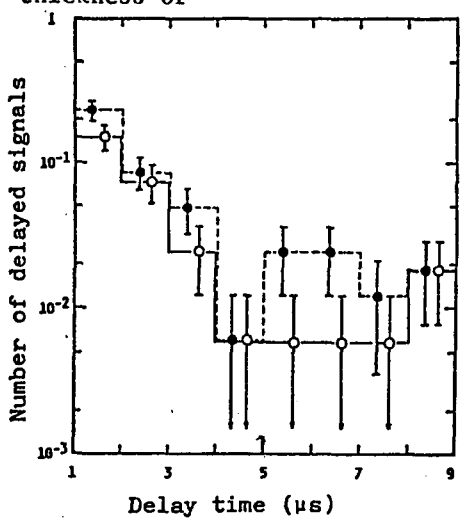

Fig 11. Delay time distribution of signals delayed by longer than 1 μs. Filled circles >0.5 particles. Open circles > 1 particle. (HE 4.7-5)

The Linsley method utilising Disk Thickness at Large Core Distances

The technique depends on σ_t or some equivalent being a

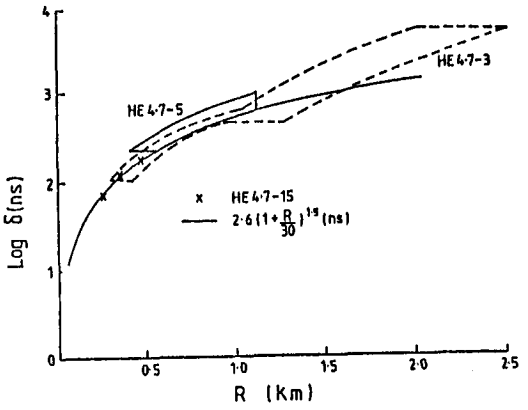

Fig 12. Arrival time dispersion of particles in the shower front.

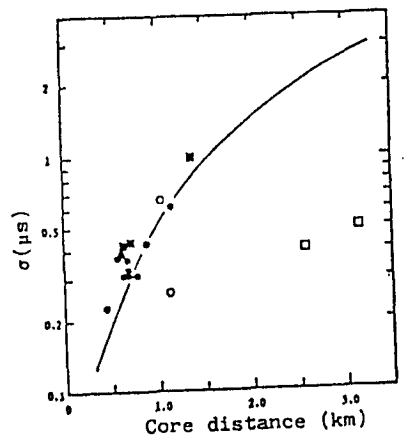

Fig 13. Time dispersions (σ) of the arrival time distributions of particles. The number of particles observed in the unshielded detectors:
filled symbols >10
open symbols <10.

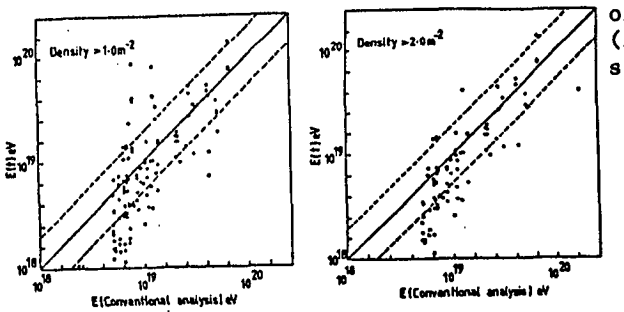

Fig 14. Plots of energy derived from risetime against energy derived from conventional analysis. (HE 4.7-6)

reliable thickness parameter at large core distances. There appear to be some late "sub-luminal" pulses associated with showers (fig 11) which are not just an extended tail of the conventional shower disk (Linsley, HE 4.7-13, Kakimoto et al, HE 4.7-5). It is possible that these are due to low energy nucleons but the tail needs more investigation with a good system impulse response before one can be sure that selection effects are not causing these very late pulses to be interpreted as a separate phenomenon. The form of σ_t is such that large values of $(t-\langle t\rangle)$ are given considerable weight and there is a need for theoretical studies to search for a suitable alternative parameter which is more linear in $(t-\langle t\rangle)$ so that a few delayed particles can not dominate the parameter.

Measurements have been made of the disk thickness at large core distances (fig 12) by Akeno and Moscow workers (HE 4.7-3/5/15) and the Haverah Park group (HE 4.7-6) investigated the Linsley technique by applying it to conventionally analysed showers. It appears that, as one might expect, agreement is best when a large number of particles is detected (figs 13, 14). Both data sets show dramatic improvements in energy estimation with increasing particle density in the detector. The Haverah Park data suggest that, for a factor of two agreement in shower energy, they would need $\gtrsim$ 64 detected

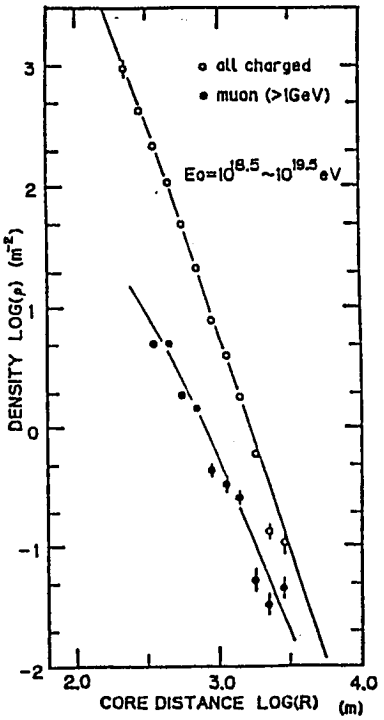

Fig 15. The lateral distribution of electrons and muons. (HE 4.7-3)

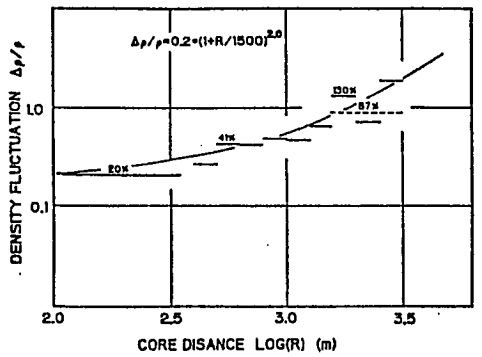

Fig 16. The fluctuation of electron densities. The broken line is derived from pulse height distribution of single particles. (HE 4.7-3)

particles ($\gtrsim 2m^{-2}$) and the Akeno group would appear to need $\gtrsim$ 10 particles for an acceptable system. It is noteworthy that at very large core distances (~2km) the technique remains to be proven and Teshima et al (HE 4.7-3) warn that an apparently steepening lateral distribution above 1km (fig 15) and large electron density fluctuations (fig 16) might finally limit the usefulness of the technique (however, Watson implied in a question that measurements of long pulses at these core distances may have caused underestimates of the density at these distances). The Akeno workers successfully used a time parameter T_{20-70} (the time between 20% and 70% of the full shower front) and such a linear parameter may well be preferable to σ_t for the reasons suggested above (fig 17). It is noteworthy that at large core distances the disk is so wide that one can reasonably expect to use simple pulse counting techniques or slow ($\lesssim$ 50MHz) sampling transient digitisers so that recording systems can be simple and economical (Ng et al, 4.7-10).

Radio Emission from Air Showers

The study of radio signals from showers might offer an inexpensive technique for constructing very large area detection arrays for giant air showers and may also provide information on shower development through the frequency spectrum of the radiation. The main period of study of radio emission was the decade from 1965-1975 but the work has continued and new results were presented at the conference. It should be remembered that interest waned in this field a decade ago through the lack of suitably large signal to noise ratios. We need to be convinced that this fundamental problem is being overcome.

Close to the shower axis, a radio system observes the shower

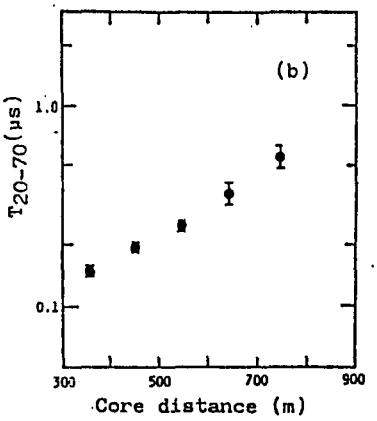

Fig 17. The average T_{20-70} of the arrival time distributions of particles. (HE 4.7-5)

with the sort of pulse widths/time periods found in fast Cerenkov work (~10ns) and the frequency spectrum thus extends typically to ~100 MHz and contains development information similar to other fast timing data. As one moves away from the axis, time compression is lost and the shower signal is observed over the full tens of microseconds of observed shower development. A frequency spectrum is then produced with important components at tens of kilohertz.

In order to make effective use of the radio technique one needs both a solid theoretical foundation and a good signal-to-noise ratio. In the VHF band, say 20 MHz to 150 MHz, Datta and Pathak (HE 4.6-4) have confirmed that we understand reasonably well the emission mechanism in terms of known charges and their motion within the shower. At low frequencies ($\lesssim$ 1 MHz) the situation has never been clearly resolved. The observed amplitude spectrum increases with decreasing frequency and there have been reports of large variations in field strengths, perhaps associated with local conditions.

Suga and his co-workers (HE 4.6-3) have begun a new attack on the low frequency region (50 kHz to 1 MHz) in conjunction with the Akeno array and have confirmed that there are large pulses to be detected from giant showers out to ~ 2 km and that these pulses are stable under varying local conditions (fig 18). This experiment is in development and use is being made of modern techniques to obtain the best possible signal to noise ratios. The current situation is that large pulses are observed but not with really large signal to noise ratios. At ~ 1 km one appears to require a 10^{10} particle shower to obtain a signal to noise $\geq$ 10:1. This is not adequate for a stand-alone system in a time-varying noise environment and more development is needed. Also, the radio emission mechanism is not yet clear at these low frequencies. Datta and Pathak were unable (along with many predecessors) to satisfactorily account for

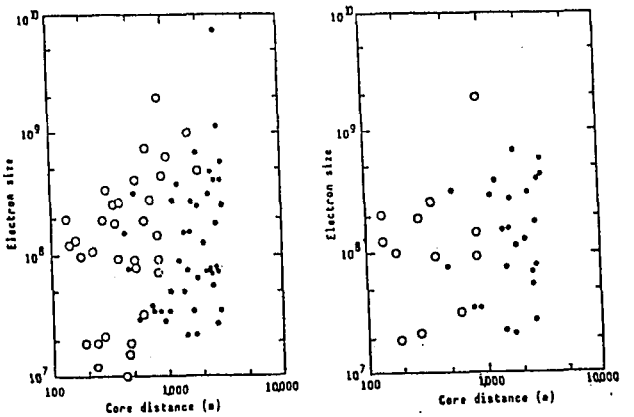

Fig 18. Air showers accompanying radio signals observed well beyond the background noise (open circles). Unaccompanied by radio signals (filled circles).

the observed field strengths (several mV. m^{-1} in a 10^9 particle shower at 1km) in terms of conventional emission mechanisms. These difficulties are of long-standing and are particularly perplexing since the problem is conceptually straightforward:- a current of $\sim 10^8$ electrons, viewed from~ 2km as it builds up and decays from ~10km to the ground.

Nishimura (HE 4.6-15 corrected in oral presentation) has specifically considered emission mechanisms in the low frequency/large core distance range and showed the dominance here of the shower negative charge excess due to positron annihilation in flight. As this number changes with altitude (or observed time), there is strong observed low frequency emission. Also, when the charges effectively disappear from the observer as the shower hits the ground, there is a process like transition radiation which gives coherent radiation preferentially at low frequencies (due to the typical time scale of the shower disk absorption of ~ 0.1 to 1 μs). At core distances of ~1km, the charge excess and transition radiation contributions should be comparable and produce a total field strength similar to (or perhaps a little below) that observed by Suga et al. In principle, the radio lateral distribution should be quite broad at low frequencies since coherence will not be lost. If a serious stand-alone system is to be developed, the impulsive time-variable background will present major problems and also some shower direction finding method will be needed if anisotropies are to be studied. Bandwidths of ~10^4 Hz preclude conventonal fast timing although it may be possible to use phase measurements for this purpose.

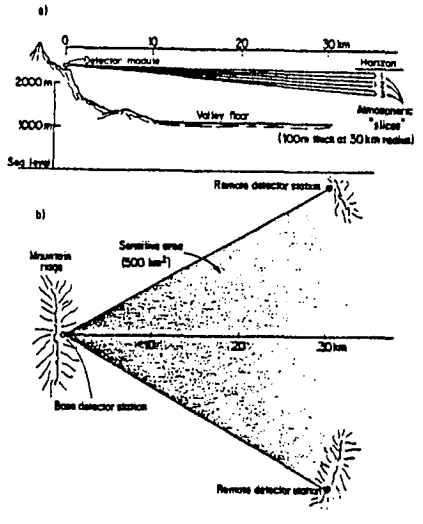

Fig 19. Proposed side-looking air fluorescence detector to observe $E_o > 10^{19}$eV air showers. (HE 4.6-6)

Air Fluorescence Techniques

Halverson and Bowen (H.E. 4.6-6) are studying the use of air fluorescence light produced near ground level by giant air showers as a basis for cheap large-area arrays. The idea involves looking down into large valleys or canyons to see fluorescent light from distances up to 35 km against a dark mountain background rather than against the relatively bright night sky (fig 19). The general properties of fluorescent light for air shower work have been proven by the Fly's Eye group and one should have confidence in the potential of the technique. To be useful however, a cheap detection system is needed and it is proposed to use cylindrical mirrors which view broad "slices" almost horizontally across the valley. Timing and amplitude measurements from perhaps three systems will contain information on the shower direction and size. However, the proposed slices are rather close together to ensure that all viewing is kept within the valleys and it would seem unlikely that good fast timing directions will be obtained vertical "baseline" of only a few hundred metres.

It is proposed that light detection will be through bars of

acrylic strips (fig 20) doped with wavelength-shifter to make good use of the ultraviolet component remaining in the light reaching the detector. The bars then act as light guides to photomultipliers. Since internal reflection at the surface is important, it may be necessary to take particular care in using such a system in a dusty desert environment which might cause progressive surface damage. Protection from unwanted local lights may be necessary.

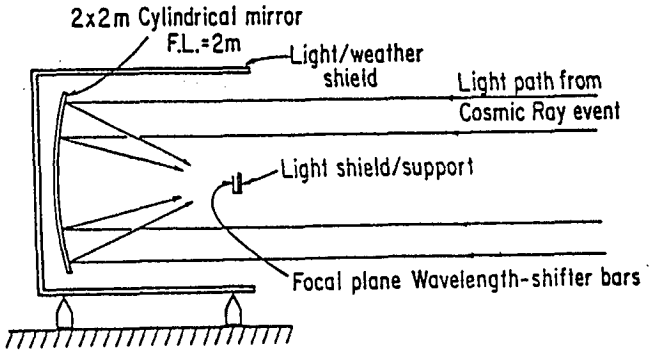

Fig 20. Side view of proposed side looking detector station. (HE 4.6-6)

5. Gamma Ray Initiated Showers

The discovery by Samorski and Stamm (1983a) of point sources of cosmic ray showers has predictably brought renewed interest in the properties of gamma ray initiated showers. One would like to have some way of picking out likely gamma ray showers from a conventional cosmic ray background and one would also wish to be able to realistically assign primary energies for the observed events. The muon component of these showers is particularly perplexing since we have long expected small values of $N\mu/Ne$ to characterise gamma ray showers whereas Samorski and Stamm (1983b) apparently observed muon signals which were not much less than those expected for conventional massive particle initiated showers.

Papers presented at this conference are in agreement that muon numbers ($\gtrsim$ 1 GeV) and hadrons in gamma ray showers produced by photoproduction should be $\lesssim$ one tenth of those expected for conventional (proton initiated) showers (eg fig 21) and the ratio is even greater if iron primaries are used for comparison (Edwards and Protheroe,HE 4.5-7). Clearly $N\mu/Ne$ should be a useful selection criterion for gamma ray showers. Indeed Stanev, Vankov and Halzen (HE 4.5-3) point out that, due to large fluctuations in muon production, most gamma ray showers will have only half the average number of expected muons.

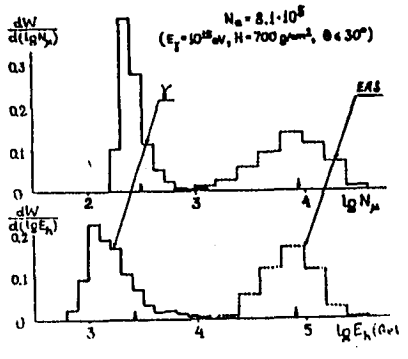

Fig 21. Expected muon number and hadron energy distributions for gamma initiated and conventional EAS. (HE 4.5-16)

The Tien Shan workers have been selecting muon-poor and hadron-poor showers as gamma-ray initiated showers and and Nikolsky et al (HE 4.5-11) have studied showers detected in this way. Through calculation and a comparison with observed muon-poor showers, Stamenov et al (HE 4.5-10) showed that theory and experiment were in agreement that, at that their altitude, $(N\mu_\gamma/N\mu_A) < 0.15$ and

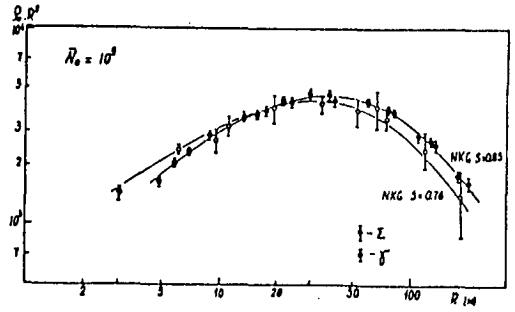

Fig 22. Electron lateral distributions measured for conventional and potential gamma initiated EAS. (HE 4.5-11)

(hadron energy/electron energy) $\lesssim 1.5 \times 10^{-2}$ were good selection parameters for such showers. A study of Tien Shan electron lateral distributions was made by Nikolsky et al. They found that muon-poor (electromagnetic?) showers were steep near the core as expected since secondary hadron transverse momenta were not involved. They also found that, at this altitude, the overall electron lateral distributions at large core distances (fig 22) were also slightly steeper for pure electromagnetic showers ($S = 0.76 \pm .02$) compared to "normal" showers ($S = 0.85 \pm 0.1$). This may be a true development effect. It is noteworthy that, since we expect gamma-ray showers to have smaller development fluctuations than background proton showers, old shower age may still be a useful gamma selection parameter since selection would tend to be against a background of young downward fluctuating proton showers. Hillas (HE 4.5-6) has calculated shower parameters for proton and gamma ray intiated showers at sea level. Again, a factor of ten is typical of the reduction in muon numbers for gamma ray showers (fig 23). He showed that a measurement of the ratio of signal in a deep water Cerenkov detector to a (5cm) scintillator detector can also provide a practical way of selecting an equivalent to muon-poor showers at large ($\gtrsim$100m) core distances (fig 23). As one might expect with a low muon content, gamma-ray showers produce a steeper lateral distribution for the deep detector, particularly at large core distances ($\gtrsim$ 100m).

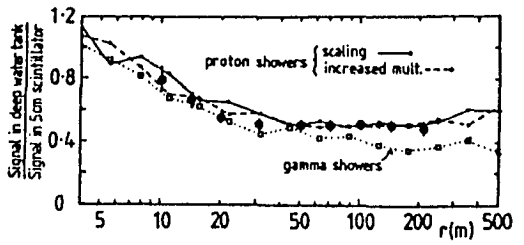

Fig 23. Ratio of particle densities recorded by two detectors in proton and gamma showers at various axial distances. (Sea level). (HE 4.5-6)

There is agreement that without the addition of some new physics to the calculations, the problem of the Kiel muon result remains. Hillas attempted to see how far one can move from conventional photoproduction to generate pions and muons more readily and still obtain results which fit conventional showers. In his model, he arbitrarily increased the hadronic cross section for photons above 1 TeV. This gives many more muons, and the required number of muons for the Kiel "gamma ray" showers can be produced. It is remarkable and salutory to note that Hillas was able to show that such an unconventional novel interaction model could still give a conventional N_μ vs N_e relationship for conventional showers (this is presumably necessary since the Kiel group have not found strange muon properties for conventional showers) and also gives a good fit to their lateral distribution functions.

It is possible that gamma-ray showers might have produced

effects in Samorski and Stamm's muon detector which fitted selection criteria for muons but were due to some other process. Stanev, Gaisser and Halzen (reported in HE 4.5-1 but withdrawn) suggested that at ~10m from the core photons might "punch through" the 880 gcm^{-2} of concrete shield and produce a signal in flash tube detectors. Blake and Nash (HE 4.5-1) investigated this possibility with data from their muon detector at Haverah Park. Their data were for core distances >20m and showed that here, "punch through" for 10cm and 20cm of lead was insignificant (fig 24). However they also used a data set of "local showers" and 20cm of lead shielding to show that below ~10m, the typical distance of the Kiel measurements, significant punch through accompanied their muons (~2:1).

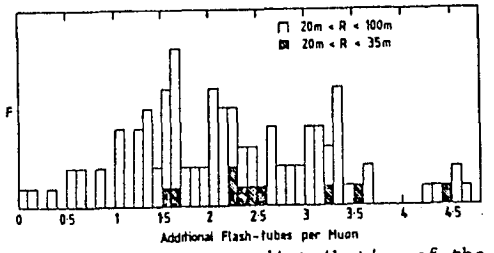

Fig 24. The frequency distribution of the electron accompaniment per muon capable of penetrating at least 5cm of lead. (HE 4.5-1)

In their presentation, Stephens and Streitmatter (HE 4.5-5) commented that, if they included incomplete screening in their calculations, pair production by low energy ($\lesssim$10MeV) gamma rays would be suppressed leading to a build up of relatively penetrating particles. It remains to be seen whether, if this is correct, the Kiel workers would have observed any effect with conventional showers but the result emphasises the need for calculations to follow the electromagnetic component correctly to the lowest possible energies.

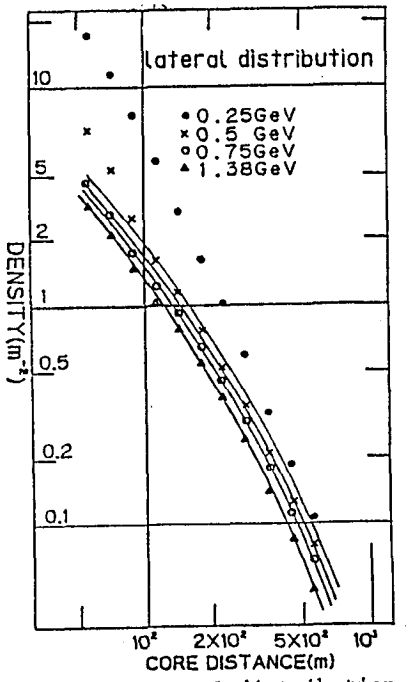

Fig 25. The lateral distribution of the density of muon signals at each layer of absorber for vertical showers. Curves are those given by the Greisen formula with R_0=280m. (HE 4.3-8)

The Akeno group has been studying the penetration of muons through concrete absorber (Matsubara et al, HE 4.3-8) and has found that at small core distances, there is a deviation from a conventional muon lateral distribution function which has a lateral distribution rather like the electromagnetic component suggesting a "punch through" effect (fig 25). This leakage occurs below 500m for 0.25 GeV threshold muon detectors, and below 150m for 0.5 GeV detectors (shower

size 10^7 particles) and may be consistent with the Kiel observation at 880 gcm^{-2} of concrete and core distances <10m.

Evidence for Low-Muon Gamma Showers

Despite the Kiel finding that there were muon-like signals associated with their gamma ray events, a muon-poor criterion has been applied apparently successfully by other groups. Akeno workers (OG 2.1-5) have observed events from Cygnus X-3 only when they applied a muon-poor content cut (set at N_μ/N_e <0.001 compared to a mean for all events of 0.03). It is noteworthy that the muon measurements in this case were made at rather large (> 50m) core distances. Kaneko et al (OG 5.3-2) appear to have confirmed the Adelaide Vela X-1 observation with muon-poor showers recorded many years ago at Chacaltaya. Kirov et al (OG 2.3-3) found an excess of events from the direction of the Crab Nebula only when a muon-poor ($N\mu/\overline{N\mu} \leq 0.11$) cut was applied. On the other hand, Blake et al (OG 2.1-4) were unable to find any evidence for a lack of muons in events from the direction of Cygnus X-3 and at the phase peak. The position is then not yet clearly for or against muon-poor astronomy.

6. The Shower Front at Small core Distances

The shower front has a thickness which increases with core distance. This allows us to study aspects of shower development through disk thickness measurements at large distances where there may also be a separation of the muon and electromagnetic fronts. At small core distances, the disk is very thin and until recently there has been a general contentment to leave it at that. However, technology for studying fronts a few nanoseconds (x c) thick is now readily available and there are also now pressing needs for such measurements. We would like to understand the Linsley broadening better, there is interesting evidence for shower front structure, and ultra high energy gamma ray astronomy requires improved angular resolution through better shower front timing.

Woidneck and Bohm (1975) provided basic data by sampling the shower front and found typical thicknesses of 2 nanoseconds (x c). At this conference, Sasaki et al (HE 4.7-1) and Inoue et al (HE 4.7-2) gave more detailed information directly from the risetime and full width at half maximum of observed scintillator pulses. The longitudinal widths were derived by correcting the observed average signal shapes for the system impulse response (fig 26). If the impulse response removal proves correct, these widths are very narrow ($\lesssim$ 2ns at 20m from the core) and seem rather narrower than measured by Woidneck and Bohm. If the fronts of gamma ray initiated showers are this narrow, one

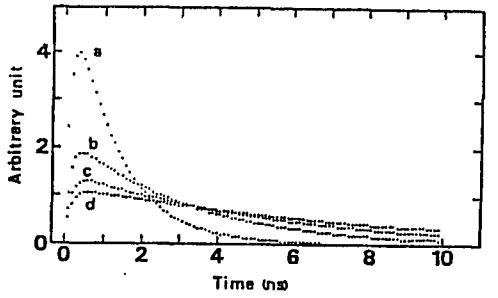

Figure 26 Corrected arrival time distributions of air shower particles for showers with sec θ of 1.0-1.2 and
(a) Ne of $3.2 \times 10^{5.5}$ - $1.0 \times 10^{6.0}$ for core distances 10m-20m
(b) Ne of $1.0 \times 10^{6.0}$ - $3.2 \times 10^{6.5}$ for core distances 20m-30m
(c) Ne of $3.2 \times 10^{6.5}$ - $1.0 \times 10^{7.0}$ for core distances 30m-40m
(d) Ne of $1.0 \times 10^{7.0}$ - $3.2 \times 10^{7.5}$ for core distances 40m-50m

might hope that shower front sampling for small U.H.E. gamma ray telescopes might not be a serious factor in limiting the array fast timing angular resolution.

Calculations on shower front thickness were presented by Nakatsuka (HE 4.4-11/12, HE 4.7-11). These were the first such calculations for some years and generally confirmed the recent observations. It is interesting to see how narrow the disk may be at the smaller core distances and also that this thickness depends a little (inversely) on distance to shower maximum (fig 27). These are results of considerable current interest and we need to see whether or not they are confirmed by more complete shower models and calculations.

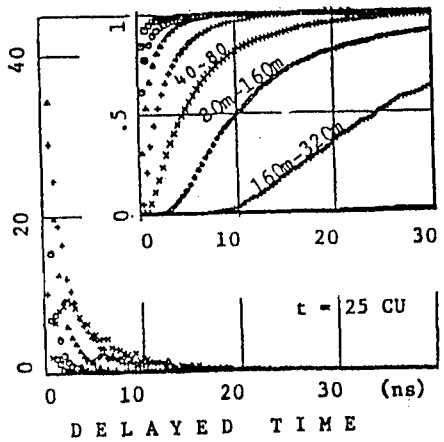

Fig 27. The arrival time structure at various distance from the axis. The distances are 0-5m, 5-10m, 10-20m,etc., (HE 4.7-11)

Structure in the Shower Front

Shower front observations sometimes show delayed structure which is correlated among a number of nearby detectors. These delayed sub-showers were discussed by Sasaki et al (HE 4.7-1) and Kamamoto et al (HE 6.2-10) and delays of a few tens of nanoseconds have been observed (fig 28). The delayed pulses do not seem to be instrumental or sampling effects on the basis of simulation of the detection procedure. Also, Sasaki et al have been able to identify delayed pulses with multiple core structure observed with the Norikura system. This interesting but difficult work is still severely limited by instrumental time resolution.

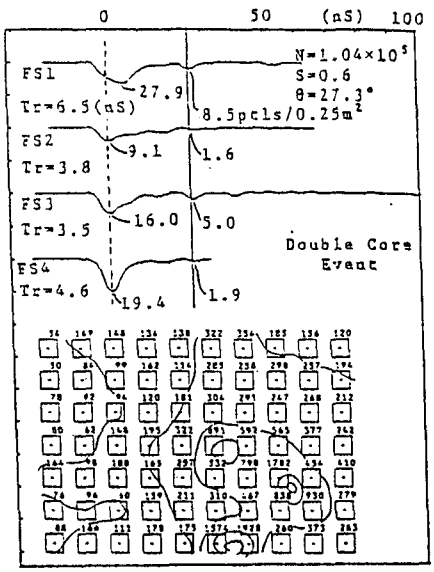

Fig 28. A multicore event showing subpeaks delayed similarly in a number of detectors (HE 4.7-1)

7. Mini-Arrays

The Hong Kong and Michigan groups have been working on the practical implementation of the Linsley array concept. In order to be successful the designs must be simple and inexpensive or the original intention will be lost. There is the need to ensure that whatever results are obtained on anisotropies and spectra will be acceptable in comparison with data obtained by more conventional means. If the technique in

principle is possible, that is the shower front width proves to be an acceptable parameter, then suitable practical means of triggering, density measurements, and direction measurement must be found.

Triggering for a Linsley array requires pulse width discrimination. Hazen and Hazen (HE 4.7-7) assume that, for a broad shower front, individual particle arrivals will be resolved and a pulse counting system in a 2μs window can give a suitable trigger (with a pulse dead time of 30-40ns). The concept of digital discriminators in this sense is new and discrimination can be done either in software or by reconstructing an analog amplitude. With such a system, it is not possible to use the discriminator output for fast timing purposes but the pulse train itself can be used. The leading particle can be timed by a fast preamplifier/discriminator (Ng, HE 4.7-9) and the arrival time of all pulses can be stored in a fast register to be read into a microcomputer.

There is some loss of useful information in such arrangments. If there is a bunching of shower particles, amplitude information will be lost and it may be preferable with some extra expense to use a simple flash digitiser (multiple level discriminator) particularly as a large shower falling relatively close-by might saturate a leading edge discriminator for an appreciable fraction of the acceptance time and, in a worst case, may be not recognised.

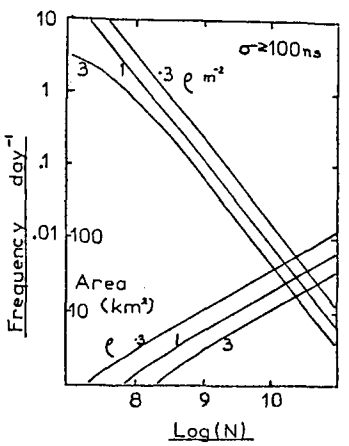

Fig 29. Expected rates for a mini array. (HE 4.7-8)

Timing for the determination of shower directions is a serious problem. With a small array, 10ns timing may not be adequate, particularly if a limited number of shower particles is spread through a ≥ 100ns front. The suggestion that track visualising detectors should be employed is being seriously studied (Ng and Chan, HE 4.5-14). An alternative being considered at Adelaide may be to use an aray of Linsley arrays in a 1km grid. Fast timing could be done in a conventional way and supplementary core location information would be available from the front width. The Linsley arrangement would reduce the data recording to $1hr^{-1}$ per detector by a reduction of the trigger rate of individual detectors. This is a cheap alternative to the two-fold local coincidence used by SUGAR.

Hazen (HE 4.7-8) has looked carefully at some practical problems of background and expected rates (fig 29). Typical rates for small (100ns) pulse widths and small (a few m^2) detector areas are ~ a few per day giving an array with a threshold of $10^{17} - 10^{18}$ eV. These rates agree well with observations made so far.

8. High Energy Muons

High energy muons are results of the early interactions in the shower and should be sensitive to early interaction parameters through both their total number (Wrontiak and Yodh HE 4.1-2, 4.1-7) and their lateral distribution function. Muons with energies greater than 200 GeV

have been discussed by Bazhutov et al (HE 4.3-16) and Cho et al (HE 4.3-7). Cho et al find that the lateral distribution function is much too steep for them to be anything but a proton dominated flux in their observations at 10^{14} to $10^{14.5}$ eV. Moscow results (HE 4.3-16) for showers in the size range above this show a rather broader distribution which fits better with their preferred mixed composition although particular interaction models have to be introduced to increase the total muon number and widen the lateral distribution a little. These characteristics are also associated with models of high atomic number primaries.

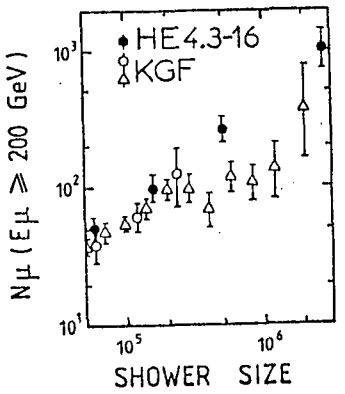

Fig 30.

Mountain altitude data (Acharya et al 1983) had indicated that, as one passed through the region of the knee, there was a reduction in muon numbers for a given Ne. A comparison of the Moscow sea level results with those data scaled to sea level failed to confirm such an effect and the source of this important discrepancy is not clear (fig 30).

9. Low Energy Muons

Lower energy muons are commonly detected in conjunction with larger air shower arrays and are studied particularly at large core distances where the muon component progressively dominates the total detector signal. The lateral distribution function, total muon number, and the muon pulse risetime are of interest in reflecting cascade development.

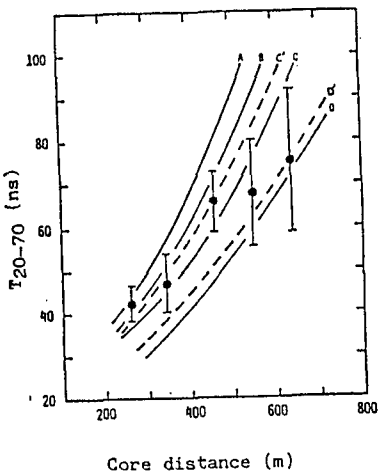

Figure 31. The average T_{20-70} of the arrival time distributions of muons with energies above 1.0GeV for showers with N_e of $10^{8.0}$–$10^{8.5}$ and secθ of 1.0-1.2 compared with those calculated from A: scaling model, B: a model with an $E^{1/4}$ multiplicity law, C: a model with an $E^{1/2}$ multiplicity law and D: a model with an enhanced $E^{1/2}$ multiplicity law and with first-interaction depths of 40gcm^{-2} for A-D and 120gcm^{-2} for C'-D'.

Muon arrival time data were reported by the Akeno (HE 4.7-4) and Haverah Park groups (HE 4.3-10). Taking into account details of the experimental arrangments (system response, muon energy threshold etc), the agreement between these experiments is good. However, agreement with the model used by McComb and Turver (private communication (1981) quoted in HE 4.3-10) is very poor, with extreme models being required to fit the data. Kakimoto et al suggest that their muon (>1GeV) risetime data indicate an early fast development of showers (Ne ~ 10^8) since the muon risetime results as a function of core distance show rather short risetimes at large core distances (fig 31). However, this may be a measurement artefact at small muon densities and also, at the present time, the statistical uncertainties in the result do not preclude many other models. It appears also that there is no evidence in these data for any muon photoproduction of 0.5 GeV muons. If the data

are correctly interpreted, the ratio of photoproduced to all muons above 0.5 GeV must be much smaller than calculated by McComb, Protheroe and Turver (1979). There is no evidence from the Akeno data (HE 4.3-8) for any substantial changes with size of Nμ/Ne. In particular, the relationship shows no evidence for any steepening associated with an increasing contribution due to photoproduction at large shower sizes (fig 32).

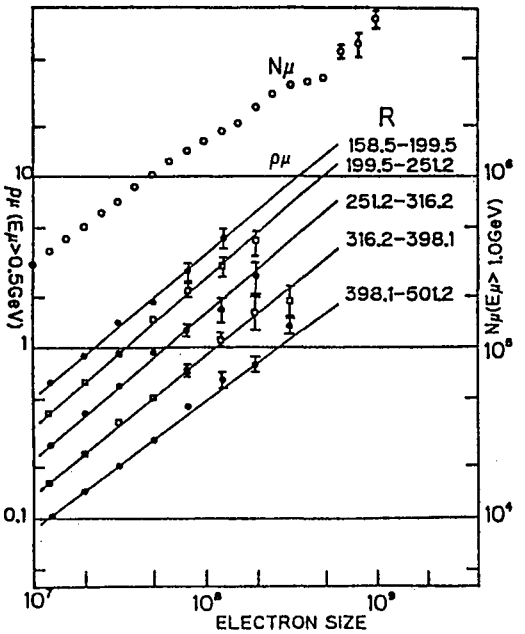

Fig 32. Size dependence of muon number and muon density. (HE 4.3-8)

Van der Walt and de Villiers (HE 4.7-12) presented some sampling statistics for shower front studies which are of interest also to those interested in shower front fast timing since the distribution of arrival times within a front probability density function determines the directional accuracy of fast timing systems. The muon lateral distributions measured at Akeno (HE 4.3-8) and Haverah Park (HE 4.3-10) are also in reasonable general agreement. At low threshold energies and smaller core distances ((0.5 GeV, <150m) and (0.25 GeV, <500m)) the Akeno group appear to find evidence for larger densities than expected. It may be that concrete shielding with depths equivalent to 0.25 or 0.5 GeV may be allowing a leakage of the electromagnetic component of the shower at the smaller core distances. This effect is shown clearly in the dependence of the observed to expected density with energy threshold and core distance. The higher the energy threshold becomes (with the sec θ absorption term), the less the leakage is observed.

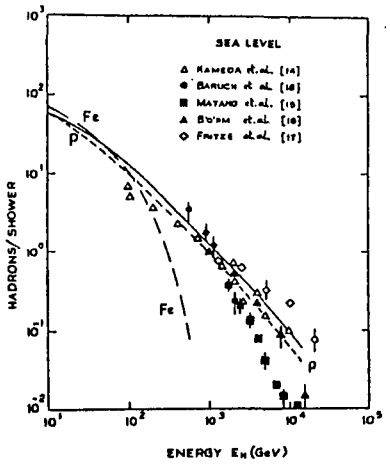

Fig 33. Hadron energy spectra. (HE 4.1-14) Dashed lines are from Grieder (1984)

10. Hadrons

In principle, studies of hadrons should give rather direct information on primary composition and early shower interactions. Indeed, there is good agreement between the various calculations presented at the conference, mainly concerning hadron energy spectra (fig 33). However, there is considerable disagreement between interpretations of experimental data. Tien Shan data can be fitted well with the calculations at nominal constant shower size but it

is not clear that in all cases proper consideration has been given in the calculations to primary energy spectra and fluctuations. Indeed, Tonwar (HE 4.1-11) has forcibly pointed out the differences between the measured parameters at various experiments (fig 34). The results depend critically

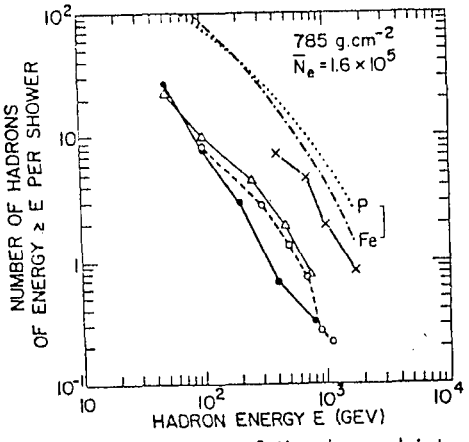

Figure 34: Comparison of the observed integral energy spectrum for high energy hadrons in air showers of average size ~1.6 x 10^5 at mountain altitudes

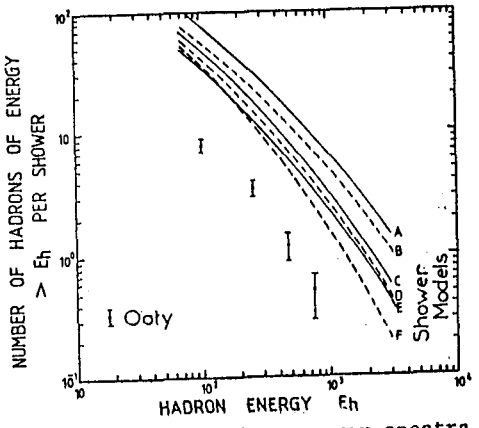

Fig 35. Measured hadron energy spectra and calculations presented in HE 4.1-11.

on how well individual hadron signals are resolved in the hadron detector. The clearest resolution, in the Tata Institute cloud chamber, gives the greatest discrepancy with calculation. Tonwar has been unable to find models which give adequate fits to the Tata data (fig 35). There is no clear route to a resolution of the discrepancies. The total experimental data as interpreted by the Tata group seems to be relatively consistent but observed high energy hadron numbers are then an order of magnitude below those expected from calculation. Conventionally measured muon and electron numbers are rather insensitive to changes in models for these highest energy interactions and discrepancies in the hadron models should not greatly affect many other air shower results.

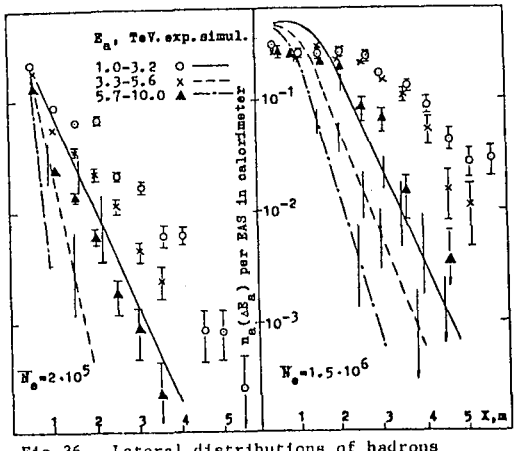

Fig 36. Lateral distributions of hadrons measured at Tien Shan compared to simulations using a scaling model. (HE 4.1-15)

Danilova et al (HE 4.1-15) examining hadron lateral distributions showed an apparent increase in large transverse momentum processes between 5×10^{14} eV and 10^{16} eV compared to those expected from lower energy accelerator p-p data (fig 36). Interestingly, the Leeds group (HE 4.2-15/16/18) have confirmed their observations of core flattening with increasing energy also in this range and thus require modification to conventional interaction models since any possible

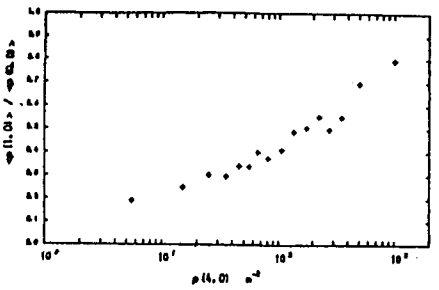

Fig 37. 'Core flattening' between 0 and 1.0m from the shower centre. The ordinate is a measure of the flatness of the lateral distribution near the core. The abscissa is a shower size parameter. (HE 4.2-10)

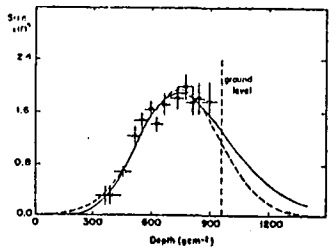

Fig 38(a). Longitudinal profile of an EAS observed by both Fly's Eye I and II simultaneously. (HE 4.4-1)

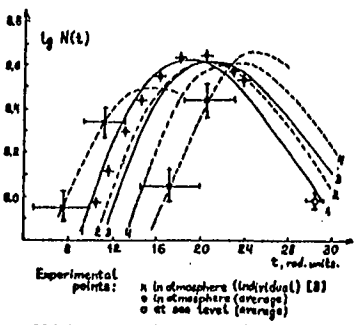

Fig 38(b). Cascade curves derived from Cerenkov pulse shape measurements. (HE 4.4-14)

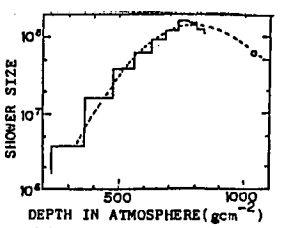

Fig 38(c). A shower curve determined from Cerenkov pulse shape. (HE 4.4-7)

composition changes appear inadequate for a straightforward interpretation of their data (fig 37). It would seem that it is necessary to ensure that a correct, broad, lateral distribution function must be included in discussions of hadron energy spectra, otherwise hadron numbers will be underestimated.

11. Cascade Functions

Many measurements we make on showers are samples of the complete shower electromagnetic cascade function. It is becoming possible to measure the complete cascade function of certain showers using atmospheric Cerenkov (Hara et al, HE 4.4-7, Fomin et al, HE 4.4-18), or air fluorescence techniques (Baltrusaitis et al, HE 4.4-1/2) (figure 38a, b, c). This study holds great promise for the next conference with the Fly's Eye group, in particular, accumulating large numbers of cascades (eg. fig 39). Already, direct measurements of E/N_{max} are becoming available for comparison with theory. The Fly's Eye group (HE 4.4-2) find

$$E_{TOT} = 1.31(\pm.14)(N_{max}/10^9)^{0.990\pm.05}$$

GeV which can be compared to the lowest value of $1.38\ N_{max}$ found in calculation by Wrotniak and Yodh (HE 4.1-2). Linsley (HE 4.4-5) has proposed the use of the function of the form

$$N = A\ \xi^q\ e^{-q\xi} \qquad (\xi = x/x_{max})$$

for fitting cascade functions and has described useful properties and applications of this function to air showers.

12. Shower Age

There is a good deal of circustantial evidence that the lateral distribution function of electrons is related to shower

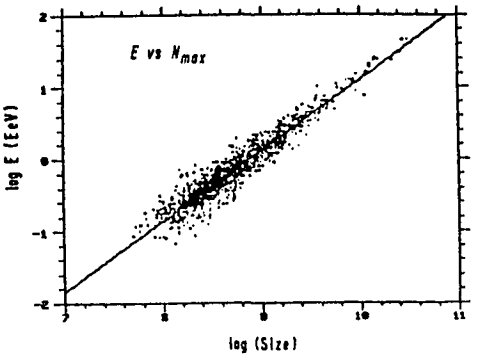

Fig 39. Scatter plot of total shower energy vs shower size at maximum as measured by the Fly's Eye. (HE 4.4-2)

development. This function, usually fitted by a N.K.G. function of age S, depends on zenith angle, shower size, (see eg., HE 4.3-4, Nagano et al 1984) and other development parameters such as the Cerenkov lateral distribution parameter b (B.R. Dawson private communication). It is unfortunate that S is not a simple parameter to use. It depends on core distance (Capdevielle and Gawin, HE 4.3-13), particularly close to the core ($\lesssim$ 10m) where it may also be affected by the transition effect, although the importance of the latter may not be great (Asakimori et al, HE 4.3-3). Close to array thresholds, the effect of selecting downward fluctuating (young) low energy showers may be seen (Chaudhuri et al HE 4.3-1).

Age probably depends on depth of maximum as $\sim 7.5 \times 10^{-4}$ per gcm (Nagano et al (1984), Fenyves et al, HE 4.3-14) and typical uncertainties are then ~0.05 - 0.07 (~70-100gcm^{-2}) so that in terms of differences in depths of maximum for iron and proton primaries discussed above, S has more potential than has yet been exploited. The problems of data sampling are now probably better understood for S than other more popular development parameters although the learning process may have damaged the reputation of age as an interesting parameter. It is particularly important to note that almost every shower can be assigned an age parameter and a data set complete in this sense is obtained.

It is not unusual to see detailed average lateral distributions fitted by NKG (S) functions for fixed shower size. I believe this process to be inappropriate because of large development (and presumably S) fluctuations for fixed Ne ; considerably distorted averages can be produced. It has been Adelaide experience in fitting lateral distributions by minimising chi-squared that the precise definition of the minimised function (in terms of observed or expected densities) can affect the fit (or absolute value of S) whilst the correct ranking in S is retained. Perhaps this should be remembered when data are compared between experiments.

13. Miscellany

Some topics in the conference are worthy of particular note as areas where progress in being made and further results should prove significant.

Constant Intensity Cuts and Attenuation Lengths

Serious efforts are being made to simulate constant intensity cuts in terms of interaction parameters and composition (Tanahashi, HE

4.1-3, Cheung and MacKeon HE 4.3-12, OG 5.2-12). This is particularly difficult for the muon component which depends on atmospheric angle as well as depth. Mixed compositions need to be simulated carefully. The use of muon data provides useful limits to the number of acceptable models.

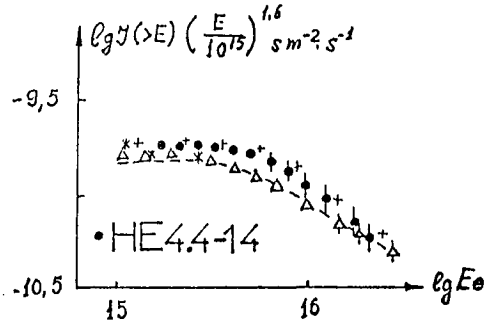

Fig 40. Integral energy spectra. The filled circles are from direct energy measurements. (HE 4.4-14)

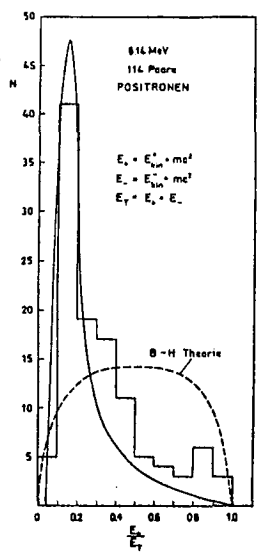

Fig 41. The positron spectrum of pairs created by 6.14 MeV gamma quanta. Note the high frequency of low kinetic energy positrons in contradiction to BETHE and HEITLER. The solid curves are as predicted by Bagge. (HE 4.4-8)

Energy Spectra

A comparison of energy and size spectra is very helpful, particularly close to the knee where detailed shape comparisons should give useful independent checks of composition models. There is a remarkable (perhaps even strange) agreement shown in HE 4.4-14 between very different techniques for deriving energy spectra (fig 40). The sharpness of spectra in Ne is often strange to me when noting that fluctuations must be taken into account.

Pair Creation Fundamentals

Bagge and his co-workers (HE 4.4-8) have been investigating deviations predicted by Bagge from the well known Bethe and Heitler theory of pair creation. The observed spectra of positrons and electrons in pair creation are shown in figure 41 and clearly deviate from the commonly assumed spectra.

Radii of Curvature

A knowledge of shower radii of curvature is important when designing fast-timing direction measurement systems. New information (fig 42) was presented in HE 4.7-15 and the radius

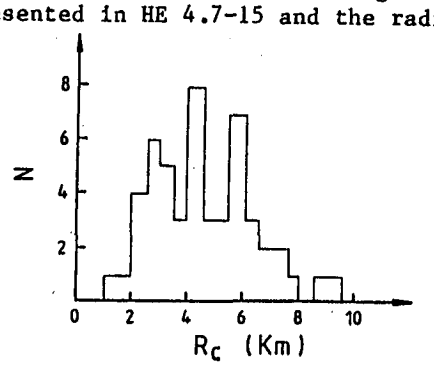

Fig 42. Shower radius of curvature distribution. (HE 4.7-15)

of curvature of the leading particles can be taken as constant at ~ 5km for core distances 200m-500m. It should be remembered that the shower front is complex with both muon and electron components and different techniques of sampling may give widely different results. As Atrashkevitch et al point out, the radius of curvature of the bulk of the particles in the shower front is likely to be much smaller, of the order of 1.5km.

Muon Charges

Moscow State University data showed no evidence for any deviation from unity of the ratio of positive and negative muon numbers.

TABLE 1

Numbers of positive I_+ and negative I_- muons.

	E_μ Gev	10-50	50-100	100-200	200-500	500-1000
r < 16 m	I_+	161	97	77	57	9
	I_-	164	91	82	56	9
r=16-32m	I_+	174	75	51	18	4
	I_-	159	68	43	15	0
r > 32 m	I_+	224	69	16	6	0
	I_-	206	61	15	6	1

14. Some Techniques

Many interesting techniques were described at the conference. Those selected below seemed to me to be particularly interesting or novel.

Fikushima et al (HE 4.2-6) described a PIN photodiode (10mm x 10mm) detection system for scintillator light from bursts (fig 43). At the present time photomultipliers are still required for small particle densities but PIN photodiode technology is clearly encroaching on their light detection area.

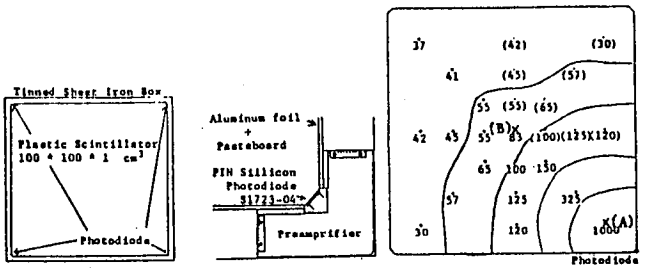

Fig. 43. Construction and uniformity of response of a scintillator burst detector using PIN photodiodes. (HE 4.2-6)

Hazen and Hazen (HE 4.7-7) described a digital "discriminator" technique for triggering when shower front particles are resolved in time and Ng (HE 4.7-9) described an antijitter constant fraction discriminator for fast timing even when these single pulses are rather slow.

Valtonen et al (HE 4.6-8) described their work on their position sensitive hadron spectrometer which should soon be operational.

Suga and his co-workers (HE 4.6-3) are studying the shape of the radio pulse (or the spectrum of radio pulses) in a rather direct way through real-time triggering of a fast fourier transform signal analyser when the shower arrives, eliminating man made frequencies from the signal, and inverting the transform to derive the original air shower pulse.

15. Some Brief Conclusions

(a) The composition shows no evidence for significant changes between 10^{15}eV (the knee) and 10^{19}eV. There is strong evidence for an early developing component and a mixed primary composition dominated by heavy nuclei when measured at constant energy.

(b) The use of shower size as an energy parameter has caused far too many problems of interpretation.

(c) The general properties of the longitudinal thickness of the shower front are well known. Linsley's suggestion of mini-arrays exploiting this parameter is worth pursuing but they will not replace conventional arrays.

(d) We cannot explain the detection by Samorski and Stamm of muon signals associated with gamma-ray showers.

(e) There is serious conflict between experiment and theory for high energy hadrons.

(f) Shower age (S) deserves more study as a shower development parameter.

(g) The measurement of complete cascade curves presents us with our best opportunity for understanding shower development.

16. References

Acharya, B.S., et al (1983) Proc 18th Int. C.R.C. (Bangalore), 9 191.
Grieder, P.K.F. (1984) Il Nuovo Cimento, 84A, 285.
Inoue, N. et al (1985a) J. Phys G: Nucl. Phys, 11, 657.
Inoue, N. et al (1985b) J. Phys G: Nucl. Phys., 11, 669.
Liebing, D.F. et al (1984) J. Phys G: Nucl. Phys, 10, 1283.
Linsley, J. (1983) Proc. 18th Int. C.R.C. (Bangalore), 12, 135.
McComb T.J.L. et al (1979) J. Phys. G: Nucl. Phys., 5, 1613.
Nagano, M. et al (1984) J. Phys. Soc. Japan, 53, 1667.
Nikolsky S.I. et al (1981) Proc 17th Int. C.R.C. (Paris), 2, 129.
Patterson, J.R., and Hillas, A.M. (1983) J. Phys. G: Nucl. Phys., 9, 1433.
Samorski, M. and Stamm, W. (1983a) Ap. J., 268, L17.
Samorski, M. and Stamm, W. (1983b) Proc 18th ICRC. (Bangalore), 11, 244.
Woidneck, C.P. and Bohm, E. (1975) J. Phys. A: Math. Gen., 8, 997.